Dynamics of viscoelastic membranes

Alex J. Levine

Departments of Chemical Engineering and Materials, University of California, Santa Barbara, California 93106
and The Institute for Theoretical Physics, University of California, Santa Barbara, California 93106

F. C. MacKintosh

Division of Physics and Astronomy, Vrije Universiteit, 1081 HV Amsterdam, The Netherlands;
Department of Physics, University of Michigan, Ann Arbor, Michigan 48109-1120;
and The Institute for Theoretical Physics, University of California, Santa Barbara, California 93106

We determine both the in-plane and out-of-plane dynamics of viscoelastic membranes separating two viscous fluids in order to understand microrheological studies of such membranes. We demonstrate the general viscoelastic signatures in the dynamics of shear, bending, and compression modes. We show that these modes remain independent in the presence of hydrodynamic interactions. The full response functions for motion both in-plane and out-of-plane are derived for the general case of viscoelastic films in contact with arbitrary viscous fluids. Specifically, we derive closed-form expressions for the in-plane longitudinal and transverse response functions for viscous membranes embedded in fluid media. We also find a screening of the otherwise two-dimensional character of the response to point forces due to the presence of the solvent.

I. INTRODUCTION

Membranes and biopolymers form many of the most basic structures of plant and animal cells. These fundamental building blocks frequently occur together in complex structures. In animal cells, for instance, the outer membrane is often strongly associated with a network of filamentous actin, one of the most prevalent proteins in the cell. This actin cortex is viscoelastic and it contributes significantly to the response of whole cells to external stress. Many prior physical studies, both theoretical as well as experimental, have concerned the structure and dynamics of simple membranes [1] and interfaces [2–5]. Much less is known about complexes of membranes with biopolymers. Recent experiments have demonstrated the ability to both construct and probe *in vitro* models consisting of lipid membranes with attached actin biopolymer [6–8]. By a microrheology technique, the material properties of these micrometer-scale viscoelastic films could be measured. Here, we calculate the dynamics of viscoelastic membranes, and thereby determine their response to external forces. We demonstrate, among other things, the general signatures of viscoelasticity in the dynamics of both shear and bend. These effects have important implications for previous and ongoing microrheological studies of both the model biopolymer-membrane complexes, as well as real cells.

Microrheology [9–14] studies the rheological properties of a material by the use of small probe particles, which can either be actively manipulated by external forces [9], or imaged while subject to thermal fluctuations. It is possible, for instance, to extract the viscoelastic moduli from observations of the fluctuating position of a small (Brownian) particle embedded in the medium [10–13,15]. The technique holds out great promise as a biological probe measuring the material properties of living cells [9]. In effect, the judicious application of this technique may permit the creation of a

''rheological microscope,'' providing insights into the regulation and time evolution of the mechanical properties of various intracellular structures over the course of the cellular life cycle, or in response to various external stimuli. Such studies of the cytoplasm are already underway [16,17]. One essential feature of the cell is the cell membrane, an essentially two-dimensional lipid bilayer incorporating a wide variety of dissolved proteins and anchored to a cytoskeletal network. Fluctuation-based microrheological studies of artificial biopolymer-membrane complexes [6,7] have been performed, and efforts are underway to extend such techniques to the membranes of real cells [18]. In order to study the rheology of the cell membrane using microrheological techniques, the previously studied methods used to extract rheological measurements from thermal fluctuations in three-dimensional samples [11–13,15,19,20] need to be extended to the problem of a viscoelastic membrane coupled to a viscous solvent [6,7].

In this paper we consider such an extension of these ideas, with an eye toward not only cellular microrheology, but also the investigation of a wide variety of systems in soft physics, wherein a viscoelastic membrane is coupled to a viscous fluid (typically water). Examples include emulsions, vesicles, and Langmuir monolayers. We calculate the position response to a force of a small rigid particle embedded in the complex, soft, viscoelastic medium. Using the fluctuation-dissipation theorem [21] we can then compute the autocorrelations of the probe particle's position—a quantity accessible in experiments. As in previous theoretical work in this field [1,6,7,12,13,19,20], careful attention must be paid to the full linear mode structure of the system. The observed thermal fluctuations of the probe particle are in response to all such modes that couple to the particle position, thus the full mode spectrum must be determined in order to interpret microrheological data. This is in distinction to more traditional rheology, which is a linear response measurement of the system to

applied shear strain and therefore measures the shear modulus directly. In particular, in this membrane study we are required to calculate the hydrodynamic flows (in the low-Reynolds-number limit) in the viscous fluid above (superphase) and below (subphase) the membrane generated by membrane distortions. The understanding of these flows is essential in calculating the modes of the combined system and, hence, the response function of the probe particle. This point has been previously recognized by Brochard and Lennon [1] in their calculation of the decay of membrane bending perturbations when coupled to a viscous fluid, and was also used in the interpretation of the recent experiments on actin-coated membranes [6,7].

Qualitatively, we find that the introduction of a viscous subphase and/or superphase introduces a new length scale over which shear waves in the two-dimensional membrane decay due to the viscous damping of the three-dimensional fluid. The appearance of a new length scale is, of course, not surprising given that the ratio of a two-dimensional membrane shear modulus $\mu(\omega)$ and a three-dimensional fluid shear modulus $G(\omega) = -i\omega\eta$ yields a length. In fact this length has been commented upon previously in the context of viscous films in contact with a viscous solvent [22,23]. In the case of membrane dynamics and microrheology, it sets a probe-particle-dependent, high frequency limit, beyond which the dynamics are controlled entirely by the solvent [6,7]. In general, this length determines a crossover length, below which the strains are two dimensional in character, and above which they are dominated by the three-dimensional fluid.

In addition to the role of membrane-liquid coupling in the shear modes, we perform a similar analysis of bending modes of the membrane. We reproduce the Brochard and Lennon results for the mode structure in the symmetric case, in which the subphase and superphase fluids have the same viscosity, and we assess the out-of-plane response function in the manner outlined briefly above. We go on to calculate the response function in this more general case of two fluids with different viscosities above and below the membrane. The asymmetric problem has clear physical relevance to the dynamics of cellular membranes as well as microemulsions. Perhaps the most dramatic example of broken symmetry occurs in the study of Langmuir monolayer dynamics. In this case, the subphase (typically aqueous) and the superphase (air) have viscosities which differ by many orders of magnitude. In the present work, we consider the general case of two fluids, above and below, with a general viscoelastic film in between [4].

Finally we point out that it is well known that in membranes whose equilibrium shapes are not flat, there is a linear coupling of bending modes to in-plane distortions due only to the nontrivial geometry of the surface [24]. We will not discuss this sort of coupling in the present work and restrict the present analysis to the dynamics of flat membranes leaving the role of curvature in microrheology to a later paper.

The remainder of this paper is organized as follows. In Sec. II we discuss the coupled modes of the membrane viscous fluid system. We use this analysis of the mode structure in Sec. III to determine the response function of a rigid par-
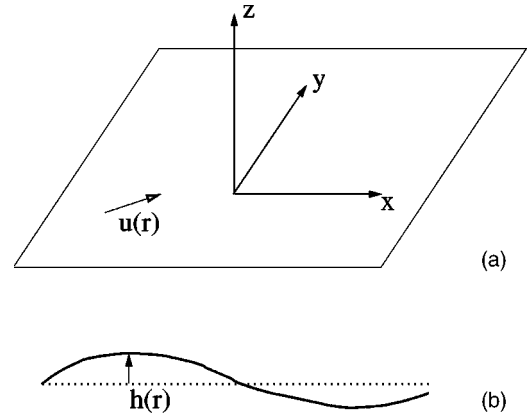

FIG. 1. The flat membrane considered in this paper. As shown in (a) the membrane lies in the xy out-of-plane coordinate system. The in-plane displacement field **u** is defined in the plane of the membrane. The fluid superphase $z>0$ and subphase $z<0$ are not shown. In (b) the edge-on view of the membrane shows the vertical displacement h of the membrane (solid line) from its flat, equilibrium shape (dotted line).

ticle embedded in the membrane in the symmetric case. We then break the subphase/superphase symmetry in Sec. IV and reanalyze the response function for the general case. Finally, in Sec. V we compute the predicted position autocorrelations of a particle embedded in a membrane whose material properties are typical of the various classes of systems mentioned above. We pay particular attention to the system of an actin-coated lipid bilayer that has been investigated experimentally by Helfer *et al.* [6,7]. We conclude and propose further experimental and theoretical work in Sec. VI.

II. THE MODES OF THE SYSTEM

We now determine the modes of the membrane coupled hydrodynamically to the (typically aqueous) subphase and superphase. The essential calculation of these involves solving the equations of motion for the fluid above and below the membrane given a certain deformation mode of that membrane. We shall do this for the three modes of membrane deformation, which we show to be independent. These modes include two in-plane modes, shear (transverse) and compression (longitudinal), as well as the out-of-plane, bending mode of the membrane. We consider first the modes of in-plane membrane deformation, i.e., those that do not involve curvature of the membrane. As long as the membrane is flat in equilibrium, these modes are linearly independent. They are also linearly independent of out-of-plane, bending deformations about a flat state.

The membrane is assumed to lie in the xy plane as shown in Fig. 1. The strain field **u** is a two-dimensional vector lying in the plane of membrane. We now need to determine the fluid velocity field above the membrane ($z>0$) associated with this shear wave. Working in the limit of zero Reynolds number, we solve the Stokes equation

$$\eta\nabla^2\mathbf{v} = \boldsymbol{\nabla}P, \tag{1}$$

where the three-dimensional vector $\mathbf{v}$ is the fluid velocity field and P is the hydrostatic pressure that enforces the fluid incompressibility

$$\nabla \cdot \mathbf{v} = 0. \tag{2}$$

These equations must be solved subject to the boundary conditions

$$\mathbf{v}(\mathbf{x}, z = 0, t) = \frac{\partial}{\partial t} \mathbf{u}(\mathbf{x}, t), \tag{3}$$

$$\lim_{z \to \infty} \mathbf{v}(\mathbf{x}, z, t) = \mathbf{0} \tag{4}$$

reflecting the stick boundary conditions of the fluid at the surface of the membrane and the requirement that the fluid velocity field go to zero at large distances from the membrane.

A. Shear deformation

We choose membrane coordinates so that the shear wave propagates in the $\hat{\mathbf{x}}$ direction and the deformation is in the $\hat{\mathbf{y}}$ direction. Thus the simple, in-plane shear deformation of the membrane is described by the strain field

$$\mathbf{u}(y, t) = \hat{\mathbf{y}} U_0 e^{i(qx - \omega t)}. \tag{5}$$

From the symmetry of the problem we look for a solution of Eq. (1) with boundary conditions given by Eqs. (5), (3), and (4) of the form

$$\mathbf{v} = -i \omega U_0 \hat{\mathbf{y}} f(z) e^{i(qx - \omega t)}, \tag{6}$$

where $f(z)$ is an unknown function satisfying the conditions $f(0) = 1$, $\lim_{z \to \infty} f(z) = 0$, so that the ansatz (6) satisfies the requisite boundary conditions. The Stokes equation demands that the vorticity of fluid flow, $\nabla \times \mathbf{v}$, satisfies Laplace's equation

$$\nabla^2 (\nabla \times \mathbf{v}) = \mathbf{0}. \tag{7}$$

Using our ansatz, we find that the unknown function $f(z)$ satisfies the differential equation

$$\frac{d^2 f}{dz^2} - q^2 f = 0. \tag{8}$$

Along with the boundary conditions given above for $f(z)$, we find a solution for the velocity field in the region above the membrane $(z > 0)$,

$$\mathbf{v}(\mathbf{x}, z, t) = -i \omega U_0 \hat{\mathbf{y}} e^{iqx - |q|z} e^{-i\omega t}. \tag{9}$$

The fluid velocity in the subphase $(z < 0)$ is similar with $z \to -z$. Returning to the Stokes equation we find that there is no pressure gradient associated with this fluid motion. We see that the shear flow induced in the three-dimensional viscous liquid phases decays over a distance comparable to the wavelength of the in-plane shear mode. This viscous damp-

ing by the surrounding fluid introduces a new decay length for shear waves in the membrane even in the case when the membrane was perfectly elastic, i.e., $\mu(\omega) = \mu_0$, a real constant. This will be discussed later. We now turn to the other in-plane mode of the membrane, the longitudinal or compression mode.

B. Compression mode

We now apply a longitudinal compression wave in the membrane having a strain field

$$\mathbf{u}(\mathbf{x}, t) = \hat{\mathbf{x}} U_0 e^{i(qx - \omega t)} \tag{10}$$

and determine the associated fluid velocity field in the superphase $(z > 0)$.

From an examination of the fluid flow near the fluid/membrane boundary, we note that the compression mode injects a sinusoidally varying vorticity field that is directed along the $\hat{\mathbf{y}}$ axis and is varying in the $\hat{\mathbf{x}}$ direction. Since the vorticity must satisfy the Laplace equation [Eq. (7)] and since the boundary conditions require it to vary sinusoidally in the $\hat{\mathbf{x}}$ direction, the fluid vorticity must decay exponentially into the fluid, i.e., in the $\hat{\mathbf{z}}$ direction. Based on these considerations, we expect that the vorticity $\mathbf{\Omega} = \nabla \times \mathbf{v}$ takes the form

$$\mathbf{\Omega} = \tau^{-1} \hat{\mathbf{y}} e^{iqx} e^{-|q|z} \tag{11}$$

in the superphase. The fluid velocity must vanish at large distances from the membrane so we have chosen a decaying exponential in the $\hat{\mathbf{z}}$ direction in Eq. (11). The constant τ, with dimensions of time, is as yet undetermined. It will be selected to enforce the stick boundary conditions of the fluid at the membrane's surface. From the above equation and incompressibility we find the differential equation obeyed by the z component of the fluid velocity field in the superphase,

$$(\partial_x^2 + \partial_z^2) v_z = -i \frac{q}{\tau} e^{-|q|z} e^{iqx}. \tag{12}$$

Once again, we use the ansatz for v_z: $v_z(x, z) = -i f(z) e^{i(qx - \omega t)}$ and find a differential equation for $f(z)$ of the form

$$\frac{d^2 f}{dz^2} - q^2 f = \frac{q}{\tau} e^{-|q|z}. \tag{13}$$

The boundary conditions at the membrane and at infinity require that $f(0) = \lim_{z \to \infty} f(z) = 0$.

The homogeneous solution of the above boundary condition vanishes upon the application of the boundary conditions on $f(z)$. This leaves only the particular solution to give the solution for v_z in the superphase. Integrating the fluid incompressibility equation, Eq. (2), then gives the accompanying solution for v_x. We find the fluid velocity to be given by

$$v_x(x, z, t) = -i \omega U_0 [1 - |q| z] e^{-|q|z} e^{i(qx - \omega t)}, \tag{14}$$
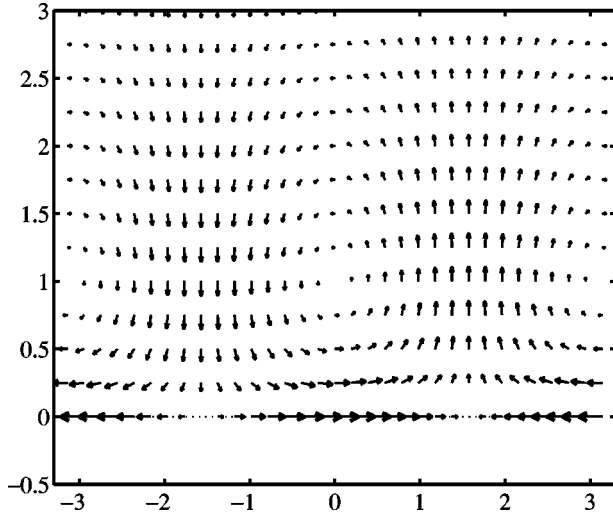
FIG. 2. The membrane compression mode with associated flow field in the superphase. The membrane, seen edge-on as a dotted line, undergoes a compression wave of wavelength 2π. The vector field represents the fluid flow in the superphase and shows the exponentially decaying vorticity.

$$v_z(x,z,t) = -\omega U_0 qz e^{-|q|z} e^{i(qx-\omega t)}. \tag{15}$$

Returning to the Stokes equation we can calculate the pressure field associated with the above flow. It is interesting to note that there is a sinusoidally varying pressure field at the surface of the membrane. We find that, for the compressional wave in the membrane introduced above, the pressure at the upper surface of the membrane ($z \to 0^+$) takes the form

$$P(x,t) = -2\eta\omega q U_0 e^{i(qx-\omega t)}. \tag{16}$$

It appears from the hydrodynamic flow field shown in Fig. 2, and from the pressure field calculated above in Eq. (16) that there should be a membrane deformation along its normal accompanying the membrane compression mode. Of course, in the symmetric case where the fluids in the superphase and subphase are identical, such a normal deformation must vanish by symmetry. As soon as this symmetry is broken, however, there should be a membrane height fluctuation in response to the longitudinal modes of the membrane. This is, in fact, incorrect. A complete calculation of the zz component of the fluid stress tensor at the surface of the membrane shows that the pressure term is exactly canceled by the viscous stress arising from the gradient of the upward fluid velocity. Thus, there is no linear, hydrodynamic coupling of this compression mode to the bending of the membrane. There will, however, be a coupling of shear and bending modes in membranes with finite mean curvature [24].

C. Bending mode

In this section we recapitulate the results of Brochard and Lennon on the effect of hydrodynamics on the dynamics of membrane bending modes. To do this we apply a sinusoidal height fluctuation to the membrane of the form

$$h(x,t) = h_q e^{i(qx-\omega t)}, \tag{17}$$

where $h(x,t)$ measures the displacement of the membrane surface in the direction normal to its surface, i.e., the $\hat{\mathbf{z}}$ direction. See Fig. 1. Once again, using the Stokes equation we calculate the fluid flow in the superphase generated by such a membrane displacement. The vorticity generated by the membrane motion must still satisfy Laplace's equation; the symmetry of the problem admits flows only in the xz plane. We assume that the solution takes the form

$$\mathbf{v}(x,z,t) = [v_x(z)\hat{\mathbf{x}} + v_z(z)\hat{\mathbf{z}}] e^{i(qx-\omega t)}. \tag{18}$$

Using the Laplace equation for the vorticity and the incompressibility condition we find two differential equations for the unknown functions $v_x(z), v_z(z)$,

$$iqv_x(z) + \frac{dv_z}{dz} = 0, \tag{19}$$

$$\frac{d^3 v_z}{dz^3} - iq\frac{d^2 v_z}{dz^2} - q^2\frac{dv_x}{dz} + iq^3 v_z = 0. \tag{20}$$

Combining Eqs. (19) and (20) in order to eliminate v_x, we arrive at a differential equation governing v_z alone,

$$\frac{d^4 v_z}{dz^4} - 2q^2\frac{d^2 v_z}{dz^2} + q^4 v_z = 0, \tag{21}$$

which has the solution

$$v_z(z) = C_1 e^{|q|z} + C_2 e^{-|q|z} + C_3 z e^{|q|z} + C_4 z e^{-|q|z}. \tag{22}$$

To satisfy the boundary condition at infinity we set $C_1 = C_3 = 0$. After integrating Eq. (19) to obtain a solution for $v_x(z)$ and applying the stick boundary conditions at the surface of the membrane, we return to Eq. (18) to write the solution for the fluid flow field in the superphase,

$$v_x(x,z,t) = -\omega h_0 qz e^{-|q|z} e^{i(qx-\omega t)}, \tag{23}$$

$$v_z(x,z,t) = -i\omega h_0 [1 + |q|z] e^{-|q|z} e^{i(qx-\omega t)}. \tag{24}$$

These flows are sketched in Fig. 3. As required, the component of the fluid velocity field tangent to the membrane vanishes.

The pressure gradient associated with the above flow field can be calculated directly from the Stokes equation. We find, upon setting the pressure to zero at infinity, that the pressure field at the surface of the membrane takes the form

$$P(x,z=0,t) = -2i\omega|q|\eta h_0 e^{i(qx-\omega t)}. \tag{25}$$

We note in passing the fact that the amplitude of the pressure oscillation is proportional to q, combined with the restoring force on the bent membrane depending on the wave vector, as q^4 leads to the well-known result that the decay rate of bending modes increases as the third power of the wave vector.
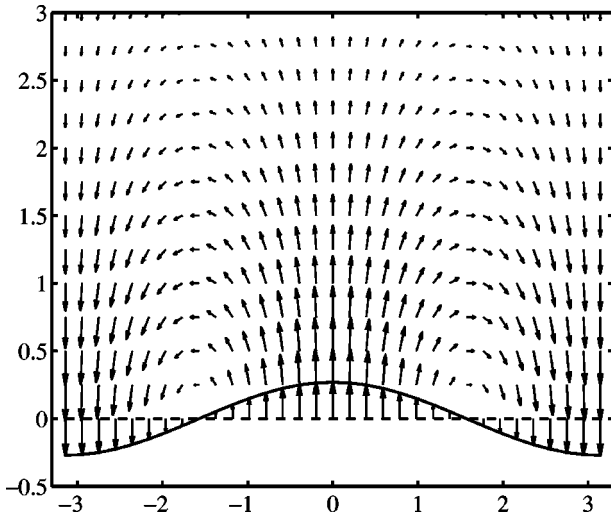
FIG. 3. The membrane bending mode with associated flow field in the superphase. The membrane, seen edge-on as a solid line, undergoes a bending wave of wavelength 2π. The undeformed membrane is shown edge-on as a dotted line. The vector field represents the fluid flow in the superphase.

III. THE RESPONSE FUNCTION

We now turn to the calculation of the response function. The calculation is similar in spirit to the calculation of the response function in three dimensions. We wish to model the response to a force of a particle embedded in the membrane at the origin. Given the level of description of the membrane, i.e., a continuum, single-component, two-dimensional viscoelastic medium, there is no distinction between the application of a force to the membrane itself over an area the size of the particle, and the application of the same force to a rigid particle embedded in the medium.

Because of our reliance on a simple, coarse-grained description of the membrane, we necessarily neglect any new hydrodynamic modes of the membrane that may, in fact, be present in the physical system. For example, if we were to consider a two-component membrane composed of lipids and an elastic protein network anchored in the lipid bilayer, there should be, in analogy to the three-dimensional gel system, a "free draining" mode associated with the diffusive relaxation of network density. Nevertheless, we expect that such modes will be irrelevant at higher frequencies, where our single-component description of a membrane should be valid for many systems of experimental interest. We defer the details related to the more complex descriptions of the membrane internal structure and their effect on microrheological measurements to a future publication. In addition we do not consider the effect of local perturbations of the membrane structure (and consequently its viscoelastic properties) due to the introduction of the probe particles. It has been shown experimentally [15,25] and theoretically [26] in three-dimensional systems that such local perturbations can be important in the one-particle response function, but that interparticle response functions do not depend on such effects to leading order.

We apply a force on the membrane that is localized at the origin of the coordinate system and is sinusoidally varying in time. We then compute the response of each Fourier mode of the membrane deformation along with the associated fluid motion. By integrating over these motions we determine the motion of the point at the origin of the membrane. The response of each Fourier mode in the viscoelastic membrane is determined from force balance,

$$0 = [\mu\partial^2 u_\alpha + (\mu+\lambda)\partial_\alpha\partial_\beta u_\beta]\delta^\perp_{\alpha i} - \delta_{iz}\kappa\partial^4 h + \sigma^{\mathbf{f}}_{iz}|_{z=0} + f_i. \tag{26}$$

In the above equation, the Greek indices run over the coordinates in the plane of the membrane, x,y, while the Latin indices run over all three coordinates. The first term in square brackets on the right-hand side (RHS) of Eq. (26) represents the in-plane membrane viscoelastic force per area due to shear and compression of the membrane. The quantity $\delta^\perp_{\alpha i}$ projects out the membrane coordinates. The membrane viscoelasticity is described by two frequency-dependent Lamé constants consistent with an isotropic continuum. These terms should in fact be expressed as integrals over the strain history of the membrane. We will, however, suppress the frequency dependence of the Lamé constants (and thus the viscoelasticity of the membrane) until we rewrite the force balance in the frequency domain. The force per unit area associated with the out-of-plane displacement of the membrane, $h(x_\alpha,t)$, is given by the second term on the RHS of the above equation, which represents the restoring force on the membrane due to its bending rigidity κ. Once again, in a viscoelastic membrane, we may assume that κ is frequency dependent, but we suppress this dependence for now.

Finally the last term on the RHS of Eq. (26) is the force per unit area exerted on the membrane by the external fluid of the subphases and superphases. The fluid stress tensor takes the well-known form for an incompressible Newtonian fluid

$$\sigma^{\mathbf{f}}_{ij} = \eta(\partial_i\mathbf{v}_j + \partial_j\mathbf{v}_i) - P\delta_{ij}. \tag{27}$$

The fluid velocity and hydrostatic pressure fields that accompany any membrane motion have been determined in the preceding section. Thus, we may rewrite the fluid stress solely in terms of the membrane displacement fields: $\mathbf{u}_\alpha$ and h. Specializing to the components of the fluid stress tensor required in Eq. (26), and noting the stick boundary conditions at the surface of the membrane, we may simplify the form of the full fluid stress tensor [Eq. (27)] to its restriction to the surface $\sigma^{\mathbf{f}}_{iz}|_{z=0}$. For a membrane immersed in a fluid medium, there are actually two such terms: one for the superphase and one for the subphase. In much of what follows, we shall consider only the superphase. It is easy to combine the effects of both, as we shall do for the final expressions of the response functions.

As we shall see, there are no linear hydrodynamic couplings of in-plane shear or compression to the bending of an initially flat membrane: a force acting in the plane of the membrane excites only the in-plane deformation modes discussed above. Similarly, the component of applied force acting along the membrane normal only generates bending deformations. Furthermore, in-plane shear and compression

retain their linear independence in the presence of hydrodynamic interactions. Using this decoupling of the in-plane and out-plane of plane modes we may calculate the response to in-plane forces and forces along the membrane normal ($\hat{\mathbf{z}}$) separately. We begin with in-plane forces.

A. In-plane response

We rewrite the force-balance equation (26), specializing to the case of an in-plane force $f_\alpha(\mathbf{x})$, and we Fourier transform it in two-dimensional membrane subspace. We arrive at

$$\mu q^2 u_\alpha(\mathbf{q},\omega) + (\mu+\lambda) q_\alpha q_\beta u_\beta(\mathbf{q},\omega) - \eta w_\alpha(\mathbf{q},\omega)$$
$$= f_\alpha(\mathbf{q},\omega), \tag{28}$$

where we have defined $w_\alpha = \partial_z v_\alpha|_{z=0}$. This actually represents only the upper half space or the superphase. For a symmetric situation with identical fluids above and below the membrane, the last term on the LHS should be doubled here, and correspondingly in Eqs. (29)–(32) below.

Projecting out the longitudinal and transverse parts of the above equation and writing $u^L = u_\alpha q_\alpha, u_\alpha^T = P_{\alpha,\beta}^T u_\beta$ with $P_{\alpha,\beta}^T = \delta_{\alpha\beta} - \hat{q}_\alpha \hat{q}_\beta$, we have

$$(2\mu+\lambda) q^2 u^L - \eta w_\alpha \hat{q}_\alpha = f(q)_\alpha \hat{q}_\alpha, \tag{29}$$

$$\mu q^2 u_\alpha^T - \eta P_{\alpha,\beta}^T w_\beta = P_{\alpha,\beta}^T f(q)_\beta. \tag{30}$$

Using the results of Sec. II, in which we have computed the fluid flows associated with the longitudinal and transverse modes of the membrane, we can determine the form of **w** in terms of **u**. In this way we can write Eqs. (29) and (30) solely in terms of **u** and thus solve for the membrane displacement in terms of the externally applied force, **f**. From the preceding section one finds

$$w_\alpha \hat{q}_\alpha = 2i\omega u^L(\mathbf{q})|\mathbf{q}|, \tag{31}$$

$$P_{\alpha,\beta}^T w_\beta = i\omega u_\alpha^T(\mathbf{q})|\mathbf{q}|. \tag{32}$$

Combining the above equations with the force-balance equations, Eqs. (29) and (30), we solve for $\mathbf{u}(\mathbf{q}) = \hat{\mathbf{q}}\hat{\mathbf{q}} u^L(\mathbf{q}) + (\overset{\leftrightarrow}{\delta} - \hat{\mathbf{q}}\hat{\mathbf{q}}) \cdot u^T(\mathbf{q})$. Thus, by Fourier transforming, one can calculate the displacement field in the membrane for an arbitrary applied force distribution $f_\alpha(\mathbf{q},\omega)$. Here, we calculate the response to an applied force localized at the origin. Specifically, we integrate over the modes of the system to determine the displacement of the point at the origin in response to the applied force at that point. The rigidity of the tracer particle at the origin is accounted for by cutting off the wave vector integral at the inverse radius of the embedded particle, $|q_{max}| \sim 1/a$, or equivalently

$$f_\alpha(\mathbf{q},\omega) = \mathbf{F}_{0\alpha} e^{-i\omega t} \Theta(q_{max} - |\mathbf{q}|), \tag{33}$$

where $\mathbf{F}_0$ is a constant vector, which for definiteness we take to be in the $\hat{\mathbf{x}}$ direction. We choose an order one numerical prefactor in this relation between q_{max} and $1/a$ so that the response function reproduces the standard Stokes drag on a

spherical particle in the limit that the membrane elasticity vanishes. Having done this, we find that the position response of the embedded tracer sphere (which is along the $\hat{\mathbf{x}}$ axis by symmetry) takes the form

$$u_x(\mathbf{x},\omega) = F_0 \int \frac{d^2q}{(2\pi)^2} \left\{ \frac{\cos^2\phi}{(2\mu+\lambda)q^2 - 4i\omega\eta|\mathbf{q}|} + \frac{1-\cos^2\phi}{\mu q^2 - 2i\omega\eta|\mathbf{q}|} \right\}, \tag{34}$$

where the angle ϕ is defined by $\hat{\mathbf{r}}\cdot\hat{\mathbf{x}} = \cos\phi$. Clearly the integral is the response function that we seek and via the fluctuation-dissipation theorem, it contains the information necessary to determine the experimentally measured power spectrum. Performing the integrals we arrive at the final form of the in-plane response function. Since it is diagonal in the in-plane indices we suppress them and write

$$\alpha_{||}(\omega) = \frac{1}{4\pi\mu} \left[\ln\left(1 + i\frac{2\mu}{3\omega\eta a}\right) + \frac{\mu}{2\mu+\lambda} \right.$$
$$\left. \times \ln\left(1 + i\frac{(2\mu+\lambda)}{3\omega\eta a}\right) \right]. \tag{35}$$

Here, and in all that follows, we use only the natural logarithm. We have chosen the wave vector cutoff here to be $q_{max} = 8/(3\pi a)$ so that in the limit of vanishing membrane elasticity, $\mu,\lambda \to 0$ with μ/λ finite, the response function reduces to the standard Stokes drag result from low-Reynolds-number hydrodynamics for a particle of radius a. Alternatively, one could require agreement with the calculated drag coefficient in Ref. [27] for a disk of radius a (and height $h \to 0$) in a thin viscous film. This requires a slightly different prefactor of order one relating q_{max} to $1/a$. Naturally, the precise prefactor depends on the detailed particle geometry.

B. Out-of-plane response

We now analyze the out-of-plane motion in a similar way by first introducing a Fourier component of the bending deformation of the membrane of the form of Eq. (17). Using our hydrodynamic results of Sec. II C in combination with Eq. (26) and computing the hydrodynamically induced stress using Eq. (27), we determine the amplitude of a bending mode of the membrane in response to an arbitrary force. We then specialize to the case of a point force and, by integrating over the available bending modes of the system, we determine the out-of-plane response of the point at the origin to a force on it directed along the membrane normal.

We make use of the fluid flow field associated with the bending deformation of the membrane as discussed in Sec. II C. From this solution and Eq. (27) we find that at the surface of the membrane there is a nonvanishing component of the fluid stress tensor, which takes the form

$$\sigma_{zz}^{\mathbf{f}} = 2i\omega\eta h_q |q| e^{i(qx-\omega t)}. \tag{36}$$

For the bending mode, the fluid stress component

$$\sigma^{\mathbf{f}}_{xz} = 2q^2\omega\eta h_q z e^{i(qx-\omega t)}, \tag{37}$$

which vanishes at the membrane. If we were to consider a membrane to have finite thickness (and thus able to support internal strains in which the deformation gradient is normal to the membrane's surface), then the bending mode would hydrodynamically couple at linear order to internal deformations of the membrane. We do not pursue this point in the current paper. For our present purposes, it is enough to note that a force normal to the plane of the undeformed membrane couples only to the bending modes.

From the z component of the force-balance equation [Eq. (26)] we find that a force in the $\hat{\mathbf{z}}$ direction with a sinusoidal dependence on x_α and t generates a sinusoidal membrane bending deformation with amplitude

$$h(q) = \frac{f_z(q)}{\kappa q^4 - 2i\omega\eta|q|}. \tag{38}$$

Integrating over such forces in q space, and determining the response to a point force at the origin using the wave vector cutoff introduced in Eq. (33) we find the out-of-plane response function

$$\alpha_z(\omega) = \frac{9\pi a^2}{2\kappa}\int_0^1 dp\, \frac{1}{p^3-i\delta}, \tag{39}$$

where the dimensionless parameter $\delta = 27\pi^2 a^3\omega\eta/(4\kappa)$ is the ratio of the viscous stress $\omega\eta/a$ to the membrane bending stress κ/a^4 at the length scale of the probe particle.

We have now completed our discussion of the response function of a bead embedded in the membrane for the symmetric case. In this case the complete motion of the particle, $\mathbf{x}(\omega)$, in the membrane is a linear combination of the in-plane motion due to the in-plane components of the applied force and the out-of-plane motion due to the component of the externally applied force normal to the membrane. Thus the most general solution of the mechanical problem to linear order in membrane displacements takes the form

$$x_i(\omega) = \alpha_\parallel(\omega)(\delta_{ij} - \hat{z}_i\hat{z}_j)f_j(\omega) + \alpha(\omega)_z f_z(\omega), \tag{40}$$

where the response functions $\alpha_\perp(\omega)$ and $\alpha_z(\omega)$ are given by Eqs. (35) and (39), respectively, and $\mathbf{f}(\omega)$ is the externally applied force responsible for the motion. We will later use the fluctuation-dissipation theorem to explicitly compute the implications of this result for the experimentally observed position fluctuations of the probe particle. First, we turn to the general case of two different fluids above and below the membrane.

IV. ASYMMETRIC SYSTEM

Here we examine the system in which the membrane separates fluids of differing viscosities. In order to study membrane dynamics in this asymmetric case we return to the question of the hydrodynamic stresses on the membrane. From our previous calculation of the fluid velocity fields associated with the various deformation modes of the mem-

brane, we determine the viscous shear stress on the membrane by demanding the continuity of the shear stress $\sigma_{\alpha z}, \alpha = x, y$ at the membrane-fluid boundary. Due to the linearity of the hydrodynamics, we can combine the solutions of the flow fields from the longitudinal (compression) and bending modes to write the full shear stress associated with a linear combination of those membrane deformations. We find that the shear stress from the fluid at the surface of the membrane may be written as

$$\sigma^{\mathbf{f}}_{\alpha z}|_{z=0} = 2\omega q_\alpha\left[i\left(\sum\eta\right)u^L(q)\right]. \tag{41}$$

Here, $\Sigma\eta$ refers to the sum of the viscosities above and below the membrane.

In a similar way we may compute the normal stresses on the membrane due to the hydrodynamic flows. The stress component normal to the membrane is

$$\sigma^{\mathbf{f}}_{zz} = 2\eta\partial_z v_z - P, \tag{42}$$

where P is the hydrostatic pressure computed from the fluid velocity field and the Stokes equation. Here we find that only the bending mode generates a nonvanishing normal stress component. The compression mode produces a pressure variation across the surface of the membrane that exactly cancels the z derivative of the vertical velocity field. We write the normal stress as

$$\sigma^{\mathbf{f}}_{zz}|_{z=0} = 2i\omega\left(\sum\eta\right)|q|h(q). \tag{43}$$

Returning to the Fourier-transformed force-balance equation we write out the components in the $\hat{\mathbf{q}}$-$\hat{\mathbf{z}}$ subspace. The $\hat{\mathbf{z}}$ equation is identical to Eq. (38). We use this result to eliminate the dependence in the $\hat{\mathbf{q}}$ equation, which takes the form

$$Bq^2u^L(q) - 2q\omega\left[i\,\mathrm{sgn}(q)\left(\sum\eta\right)u^L(q)\right] = \mathbf{f}(q)\cdot\hat{\mathbf{q}}, \tag{44}$$

where $\mathbf{f}(q)$ is the externally applied force and $B = 2\mu + \lambda$. Solving for the longitudinal part of the displacement field we arrive at

$$u^L(q) = \frac{\mathbf{f}(q)\cdot\hat{\mathbf{q}}}{Bq^2 - 2i\omega|q|\left(\sum\eta\right)}. \tag{45}$$

Combining the above result for the longitudinal part of the in-plane displacement field with the previously calculated transverse part of the in-plane displacement field as well as the out-of-plane perpendicular displacement, we can write the trajectory of any point on the membrane as

$$\mathbf{R}(x_\alpha, \omega) = \hat{\mathbf{z}}h(x_\alpha, \omega) + \mathbf{u}(x_\alpha, \omega), \tag{46}$$

which in the Fourier-transformed variables takes the form

$$R_i(q_\alpha,\omega) = \hat{z}_i h(q_\alpha,\omega) + \hat{q}_i u^L(q_\alpha,\omega)$$

$$+ (\delta_{i\beta} - \hat{q}_i \hat{q}_\beta) u_\beta(q_\alpha,\omega). \qquad (47)$$

We now calculate the one- and two-particle response functions for the asymmetric membrane using the above results. To do this, we localize the applied force at the origin by taking $\mathbf{f}(x_\alpha,\omega) = \exp(-i\omega t)\mathbf{f}\delta(\mathbf{x})$ and we calculate the displacement field of a particle attached to the membrane at some other location $\boldsymbol{\mathcal{X}}$ using the relation

$$\mathbf{R}(\boldsymbol{\mathcal{X}},\omega) = \int \frac{d^2q}{(2\pi)^2} \mathbf{R}(q_\alpha,\omega) e^{i\mathbf{q}\cdot\boldsymbol{\mathcal{X}}}. \qquad (48)$$

From this calculation we determine the response function tensor $\alpha_{ij}(\boldsymbol{\mathcal{X}},\omega)$ defined by the equation

$$R_i(\boldsymbol{\mathcal{X}},\omega) = \alpha_{ij}(\boldsymbol{\mathcal{X}},\omega) f_j(\mathbf{0},\omega), \qquad (49)$$

so that $\alpha_{ij}(\boldsymbol{\mathcal{X}},\omega)$ measures the displacement of a point at $\boldsymbol{\mathcal{X}}$ on the undeformed membrane in response to a force applied at the origin of the coordinate system. For concreteness we take the displacement vector of the observation point at $\boldsymbol{\mathcal{X}}$ to be along the $\hat{\mathbf{x}}$ axis. Then, $\boldsymbol{\mathcal{X}}$ simply represents the (scalar) separation. It is, of course, trivial to rewrite the resulting expressions in an arbitrary reference frame.

Using Eqs. (45) and (47), our previous solutions for the bending and transverse, in-plane membrane deformations in Eq. (48) we first determine the displacement of the tracer particle in the $\hat{\mathbf{x}}$ direction. The resulting angular integrals are simply written as Bessel functions and we find

$$R_x(\boldsymbol{\mathcal{X}},\omega) = \alpha_{xx}(\boldsymbol{\mathcal{X}},\omega) f_x, \qquad (50)$$

where this component of the response tensor is given by

$$\alpha_{xx}(\boldsymbol{\mathcal{X}},\omega) = \frac{1}{4\pi} \int_0^\infty dq\, q \left\{ \frac{J_0(q\boldsymbol{\mathcal{X}}) - J_2(q\boldsymbol{\mathcal{X}})}{Bq^2 - 2i\omega q\left(\sum \eta\right)} \right.$$

$$\left. + \frac{J_0(q\boldsymbol{\mathcal{X}}) + J_2(q\boldsymbol{\mathcal{X}})}{\mu q^2 - i\omega q\left(\sum \eta\right)} \right\}. \qquad (51)$$

This integral actually involves a large wave vector cutoff, which depends on the boundary conditions where the force is applied. For instance, for a force applied to a particle attached to the surface, this cutoff depends on the particle size and geometry, as described above for the single-particle response. For separations large compared with the particle size, however, we can take the upper limits of these integrals to be infinity, as we have done here. In the limiting case where one observes the displacement of the particle at the origin due to a force applied to it (the $|\boldsymbol{\mathcal{X}}| \to 0$ limit of the two-point measurement, which must reduce to the one-point measurement in this calculation), one must take into account the aforementioned cutoff for the integral.

The remaining nonvanishing components of the response function tensor are easily calculated in an analogous manner.

We find only diagonal terms, expressing the linear independence of longitudinal, transverse, and bending modes, even in the presence of hydrodynamic effects and even for different fluid viscosities above and below the membrane. The remaining components are given by

$$\alpha_{yy}(\boldsymbol{\mathcal{X}},\omega) = \frac{1}{4\pi} \int_0^\infty dq\, q \left\{ \frac{J_0(q\boldsymbol{\mathcal{X}}) + J_2(q\boldsymbol{\mathcal{X}})}{Bq^2 - 2i\omega q\left(\sum \eta\right)} \right.$$

$$\left. + \frac{J_0(q\boldsymbol{\mathcal{X}}) - J_2(q\boldsymbol{\mathcal{X}})}{\mu q^2 - i\omega q\left(\sum \eta\right)} \right\} \qquad (52)$$

for in-plane motion due to an in-plane force perpendicular to the separation vector of the two particles. For displacements normal to the plane of the membrane we find

$$\alpha_{zz}(\boldsymbol{\mathcal{X}},\omega) = \frac{1}{2\pi} \int_0^\infty dq\, q \frac{J_0(q\boldsymbol{\mathcal{X}})}{\kappa q^4 - 2i\omega\left(\sum \eta\right)q}. \qquad (53)$$

We have evaluated the response functions in a convenient coordinate system, in which $\boldsymbol{\mathcal{X}}$, the separation between the point of force application and the point at which the response is evaluated, defines the x axis. More generally, the response function $\alpha_\parallel \equiv \alpha_{xx}$ gives the longitudinal response (i.e., displacement) at one point due to a force applied at another point, where both the force and response are in the direction of the line separating the two points. Likewise, $\alpha_\perp \equiv \alpha_{yy}$ gives the transverse response, where both the force and response are perpendicular to the line separating the two points. For an isotropic membrane, there are no nonzero off-diagonal components in the plane (i.e., $\alpha_{xy} = \alpha_{yx} = 0$). For the general case of a separation vector $\boldsymbol{\mathcal{X}}$, we may define an orthonormal basis $\{\hat{\boldsymbol{\mathcal{X}}}, \hat{\mathbf{t}}, \hat{\mathbf{z}}\}$, where $\hat{\mathbf{t}}$ is chosen perpendicular to the other two. Then, the general response in-plane is given by

$$R_\beta = \hat{\boldsymbol{\mathcal{X}}}_\beta (\mathbf{f}\cdot\hat{\boldsymbol{\mathcal{X}}})\alpha_\parallel + \hat{t}_\beta(\mathbf{f}\cdot\hat{\mathbf{t}})\alpha_\perp. \qquad (54)$$

The integrals in the expressions for the purely in-plane response in Eqs. (51) and (52) can be done in closed form. A particularly interesting case is that of a purely viscous, incompressible membrane, for which $\mu = -i\omega\eta_m$. Here,

$$-i\omega\alpha_\parallel(\boldsymbol{\mathcal{X}},\omega) = \frac{1}{4\pi\eta_m} \int_0^\infty \frac{J_0(z) + J_2(z)}{z + \beta} dz$$

$$= \frac{1}{4\pi\eta_m} \left[\frac{\pi}{\beta}\mathbf{H}_1(\beta) - \frac{2}{\beta^2} \right.$$

$$\left. - \frac{\pi}{2}[Y_0(\beta) + Y_2(\beta)] \right] \qquad (55)$$

and

$$-i\omega\alpha_\perp(\boldsymbol{\mathcal{X}},\omega)=\frac{1}{4\pi\eta_m}\int_0^\infty \frac{J_0(z)-J_2(z)}{z+\beta}dz$$

$$=\frac{1}{4\pi\eta_m}\left[\pi\mathbf{H}_0(\beta)-\frac{\pi}{\beta}\mathbf{H}_1(\beta)+\frac{2}{\beta^2}\right.$$

$$\left.-\frac{\pi}{2}[Y_0(\beta)-Y_2(\beta)]\right], \tag{56}$$

where $\beta=(\boldsymbol{\mathcal{X}}\Sigma\,\eta/\eta_m)$, the $\mathbf{H}_\nu$ are Struve functions, and the Y_ν are Bessel functions of the second kind. We note that the asymptotic behavior of both response functions, as $\beta\to0$, is in agreement with Ref. [27], where the drag coefficient is calculated for a purely viscous membrane immersed in a viscous solvent. Specifically, in this limit,

$$-i\omega\alpha_{\perp,\|}=\frac{1}{4\pi\eta_m}\left(\ln(2/\beta)-\gamma_E\pm\frac{1}{2}\right), \tag{57}$$

up to terms of order β. Here, γ_E is the Euler constant. As shown in Ref. [27], the drag coefficient for a disk of radius a in a membrane of vanishing thickness and finite viscosity η_m is given by

$$\frac{4\pi\eta_m}{\ln(2/\epsilon)-\gamma_E+O(\epsilon)}, \tag{58}$$

where $\epsilon=(a\Sigma\,\eta/\eta_m)$.

It should be noted that for large values of their arguments, $J_0(x)+J_2(x)$ is dominated by $J_0(x)-J_2(x)$, so the response function along the line of centers between the two particles is dominated by the compression modulus, while the response function for in-plane motion perpendicular to the line of centers is controlled by the shear modulus as one would expect. In the following section we turn to the fluctuation-dissipation theorem to compute the experimentally observable correlated thermal fluctuations of two tracer particles embedded in the membrane.

V. POSITION CORRELATION SPECTRA

Having computed the response function to an applied force for both single-particle and two-particle systems, we now turn to the question of what is the experimentally accessible quantity. There are two basic types of microrheological measurements that are possible. In active microrheology, the response function is directly probed via the linear response measurement of the displacement of a tracer due to a force applied either to that particle (one-particle measurements) or to another particle embedded in the membrane (two-particle measurements). The expected response functions measured in such experiments have been directly calculated in this paper. It is, however, also possible to use the correlated thermal fluctuations of particles embedded in the membrane to access the same rheological information via the fluctuation-dissipation theorem, as was done for single-particle motion in Refs. [6,7]. In this section we concentrate on such thermal fluctuation spectra of one and two particles embedded in the membrane. We find the expected one-point fluctuation spec-

tra, as determined theoretically before for bending modes of fluid membranes [28], as well as for bending and shear modes of viscoelastic membranes in Refs. [6,7]. These results are consistent with the experiments of Refs. [6,7]. Largely because of the increased interest in two-point microrheology techniques, we also examine the correlated thermal motion of two embedded particles. The quantity that we compute is

$$S_{ij}(\boldsymbol{\mathcal{X}},\omega)=\int\langle R_i(\boldsymbol{\mathcal{X}},t)R_j(\mathbf{0},0)\rangle e^{i\omega t}dt. \tag{59}$$

By the fluctuation-dissipation theorem this correlation function can be written in terms of the imaginary part of the response functions calculated above as

$$S_{ij}(\boldsymbol{\mathcal{X}},\omega)=\frac{2k_\mathrm{B}T}{\omega}\alpha_{ij}''(\boldsymbol{\mathcal{X}},\omega), \tag{60}$$

where $\alpha_{ij}''(\boldsymbol{\mathcal{X}},\omega)$ is the imaginary part of the response (in the ith direction) of a particle embedded in the membrane at $\boldsymbol{\mathcal{X}}$ to a force in the jth direction. It only remains for us to compute the remaining integrals over the magnitude of the wave vector q to determine the correlation spectra.

For concreteness we put the vector defining the separation of the particles along the $\hat{\mathbf{x}}$ direction. We first compute the correlations of the in-plane motion of the particles perpendicular to their line of centers and along their line of centers by calculating $S_{yy}(\boldsymbol{\mathcal{X}},\omega)$ and $S_{xx}(\boldsymbol{\mathcal{X}},\omega)$, respectively. In all of the following calculations we assume that the in-plane shear modulus is dominated by the real part and that this is frequency independent. In other words we consider the membrane to act like a perfectly elastic sheet. Other calculations can, of course, be performed with the formulas given above. We present these results merely as an example of the correlation functions for this particularly simple case. More complex assumptions about the viscoelasticity of the membrane, presumably based on microscopic models of the membrane, can of course be incorporated in the formalism provided, and the resulting integrals can be performed.

We may write the imaginary part of the response function in the following form for the motion perpendicular to the line of centers:

$$\alpha_{yy}''=\frac{1}{4\pi\mu\tau}\int_0^\infty dz\left\{\frac{J^-(z)}{z^2+\tau^{-2}}+\left(\frac{\mu}{B}\right)^2\frac{2J^+(z)}{z^2+\tau'^{-2}}\right\}, \tag{61}$$

where we have defined the functions $J^\pm(z)$ to be the following combinations of Bessel functions of the first kind:

$$J^\pm(z)=J_0(z)\pm J_2(z), \tag{62}$$

and τ and τ' are frequency-dependent functions of the form

$$\tau^{-1}=\frac{\omega\left(\sum\eta\right)|\boldsymbol{\mathcal{X}}|}{\mu}, \tag{63}$$

$$\tau'^{-1} = \frac{2\omega\left(\sum \eta\right)|\boldsymbol{\mathcal{X}}|}{B}. \tag{64}$$

Using the same definitions, we write the imaginary part of the response function for motion along the line of centers as

$$\alpha''_{xx} = \frac{1}{4\pi\mu\tau}\int_0^\infty dz\left\{\frac{J^+(z)}{z^2+\tau^{-2}} + \left(\frac{\mu}{B}\right)^2\frac{2J^-(z)}{z^2+\tau'^{-2}}\right\}. \tag{65}$$

The physical interpretation of τ is clear: it measures the ratio of the distance separating the two particles to the screening length of shear modes in the membrane due to the coupling to the viscous subphase and superphase. The other function τ' has an analogous meaning in terms of the compression modes of the membrane. Up to an overall scale factor, the shape of the correlation spectrum obeys a distance-frequency scaling relation, so that spectra obtained at different interparticle separations can be collapsed into a master curve by rescaling distances, so they are measured in terms of the frequency-dependent screening length. The breakdown of this scaling relation can be used as a diagnostic of the appearance some significant frequency dependence of the membrane elastic moduli.

The only distinction between the two response functions shown above is the interchange of the roles of the functions $J^\pm(z)$. The effect of this switch is that the compression response dominates the long-length scale response along the line of centers, while the shear response of the membrane controls the long-length scale response perpendicular to the line of centers. This observation is intuitively obvious. We plot the resulting correlation spectra as a function of the dimensionless variable τ in the limit that the compression modulus, $B=2\mu+\lambda$, is much larger than the shear modulus in the membrane and that the particle size is much smaller than the interparticle separation, $|\boldsymbol{\mathcal{X}}|\gg a$. The plots of the undimensionalized correlation functions, $I_{ij}=4\pi\mu^2 S_{ij}/[2k_BT(\Sigma\eta)|\boldsymbol{\mathcal{X}}|]$, are shown in Fig. 4.

We now consider the same calculation for the correlated out-of-plane fluctuations of the particles. Once again using the fluctuation-dissipation theorem with the appropriate component of the response tensor, $\alpha_{zz}(\boldsymbol{\mathcal{X}},\omega)$,

$$\alpha''_{zz} = \frac{1}{4\pi\mu\tau}\int_0^\infty dz\frac{J_0(z)}{z^6+\tau''^{-2}}, \tag{66}$$

where we have defined a new dimensionless, frequency-dependent variable in analogy to τ and τ' above. In this case, τ'' measures whether the viscous damping of the bending mode on the length scale of the interparticle separation is relevant at the frequency ω. It is defined by

$$\tau''^{-1} = \frac{2\omega\left(\sum \eta\right)|\boldsymbol{\mathcal{X}}|^3}{\kappa}. \tag{67}$$

We can write the undimensionalized correlation spectrum $I_{zz} = \pi\kappa^2|\boldsymbol{\mathcal{X}}|^6 S_{zz}(\boldsymbol{\mathcal{X}},\omega)/[2k_BT(\Sigma\eta)]$ in terms of an integral
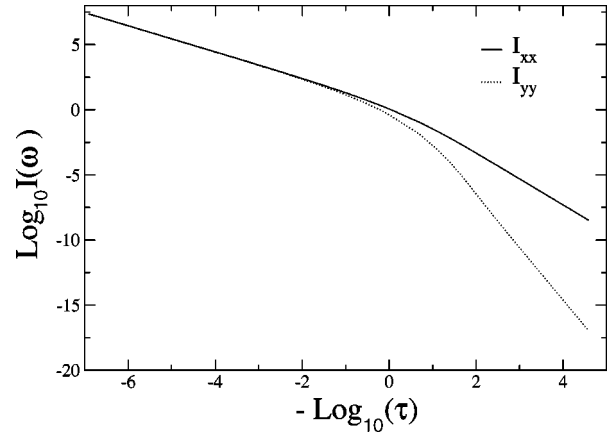

FIG. 4. The graph of the dimensionless interparticle correlation function (see text) for motion along the line of centers, I_{xx}, and motion perpendicular to the line of centers, I_{yy}, as a function of the dimensionless variable τ in the combined limits of small particle size, compared in the interparticle separation and high membrane bulk modulus, compared to the membrane shear modulus.

that is performed numerically. The resulting correlation spectrum is shown in Fig. 5, where the independent variable is τ''. It may be noted that the frequency separation scaling property of the fluctuations of the particles both along their line of centers and perpendicular to their line of centers fails for the case of the vertical motion. This breakdown of the scaling reflects the elementary result that bending energy is harmonic in the Laplacian of the vertical displacement, rather than in the gradient of the displacement field as in the case of in-plane deformation.

We now turn to one final power spectrum calculation. Unlike those discussed above, we now consider explicitly a viscoelastic membrane. Based on the work of Halfer *et al.*, we take as an example, an actin-coated lipid membrane whose viscoelastic properties are dominated by the actin coat. We further specialize to the high-frequency limit, where the actin rheology is dominated by single chain dynamics. In
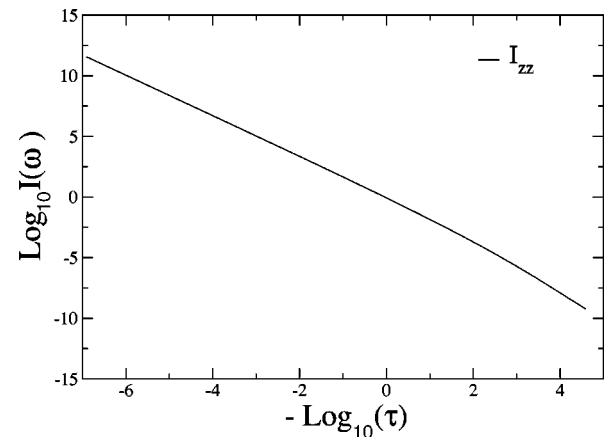

FIG. 5. The graph of the dimensionless interparticle correlation function (see text) for motion perpendicular to the membrane, I_{zz}, as a function of the dimensionless variable τ'' in the limit of small particle size compared in the interparticle separation.

this frequency range the effective shear modulus of the membrane is expected to take the form

$$\mu(\omega) = \mu_a(-i\hat{\omega})^z, \qquad (68)$$

where $z = 3/4$, μ_a is a (real) modulus scale, and $\hat{\omega} = \omega\tau$ is a dimensionless frequency. We now use the fluctuation-dissipation theorem in conjunction with the in-plane response function given in Eq. (35), in which we set the membrane shear modulus to that given above in Eq. (68) and the membrane compression modulus to infinity. This latter choice is based on the near incompressibility of the underlying lipid bilayer to which the actin network is attached.

After some algebra we determine that the single-particle power spectrum is given by

$$\langle |x(\omega)|^2 \rangle = \frac{k_B T}{2\pi\mu_a\tau^{3/4}} \omega^{-7/4} H(\omega), \qquad (69)$$

where the function $H(\omega)$ is given by

$$H(\omega) = \cos\left(\frac{3\pi}{8}\right)\arctan\left(\frac{\cos\left(\frac{3\pi}{8}\right)\beta(\omega)}{1+\sin\left(\frac{3\pi}{8}\right)\beta(\omega)}\right)$$
$$+ \frac{1}{2}\sin\left(\frac{3\pi}{8}\right)\ln\left[1+\beta^2(\omega)+2\beta(\omega)\sin\left(\frac{3\pi}{8}\right)\right]. \qquad (70)$$

The function $H(\omega)$ depends on frequency only through the dimensionless quantity

$$\beta(\omega) = \frac{2\mu_a\tau}{3\eta a}\hat{\omega}^{-1/4}. \qquad (71)$$

In the limit of high frequency (small β) it is simple to show that the power spectrum scales with frequency as ω^{-2}, as is expected for simple Brownian motion. One can show that in this limit the power spectrum takes the form

$$\langle |x^2(\omega)| \rangle \to \frac{k_B T}{3\pi\eta a}\omega^{-2} \quad \text{as} \quad \omega \to \infty. \qquad (72)$$

On the other hand, at intermediate frequencies high enough so that Eq. (68) accurately describes the membrane rheology, but low enough so that β is small, H is independent of frequency (up to logarithmic corrections) and we find that the power spectrum of the tracer particle position fluctuations decays as a different power law with frequency. In this frequency range we find that

$$\langle |x^2(\omega)| \rangle \sim \omega^{-7/4}. \qquad (73)$$

More generally, the exponent above is expected to be $-(1+z)$, where z is defined above.

We also compute the power spectrum of out-of-plane fluctuations for the membrane. This result does not depend on the frequency-dependent shear modulus of actin. Rather,

it depends on only the bending modulus of the membrane, κ, which, in principle, is also a complex, frequency-dependent quantity. In particular, for the actin-coated membrane, the bending modulus takes into account the viscoelastic result of the actin in addition to the usual bending energy of the lipid bilayer, so one should expect this quantity to have a complex frequency response. Inasmuch as this more microscopic mechanical issue has not been satisfactorily resolved, we will simply assume that the bending modulus is a real, frequency-independent quantity.

The remaining calculation, of course, is done analogously to the calculation presented above. We use Eq. (39) and the fluctuation-dissipation theorem to compute the power spectrum of $\hat{\mathbf{z}}$ fluctuations. To do so we need to consider the imaginary part of the response function by performing the integral in Eq. (39). This integral depends on the dimensionless parameter δ, which is linearly proportional to frequency. In the low-frequency limit, we find that to leading order the imaginary part of integral takes the form

$$\text{Im}[\alpha_z(\omega)] = \frac{9\pi a^2}{2\kappa}\left[\frac{\pi}{3}\delta^{-2/3} + O(\delta^{-1/3})\right]. \qquad (74)$$

From the fluctuation-dissipation theorem we then find that the power spectrum in the low-frequency limit takes the form

$$\langle |z(\omega)|^2 \rangle = \frac{1}{3}\left(\frac{2\pi^2}{\kappa\eta^2}\right)^{1/3} k_B T \omega^{-5/3}. \qquad (75)$$

Note that the above result is independent of tracer particle size. The power-law decay of fluctuations with the exponent 5/3 has already been calculated by Zilman and Granek [28] for the case of a pure fluid membrane. For a viscoelastic membrane, the overall exponent of frequency is expected to be $(5+z)/3$ [6,7].

In the high-frequency limit, the effect on the tracer of the membrane bending stress on the dynamics is dominated by the viscous stress coming from the fluid. The power spectrum for the Brownian fluctuations of the bead reduces to that of a *free* Brownian sphere,

$$\langle |z(\omega)|^2 \rangle \to \frac{k_B T}{3\pi\eta a}\omega^{-2} \quad \text{as} \quad \omega \to \infty. \qquad (76)$$

The full power spectrum of the out-of-plane tracer particle fluctuations is shown in Fig. 6; this plot demonstrates the crossover from the low-frequency, bending stiffness dominated dynamics, to the high-frequency dynamical regime controlled by the viscous stresses in the surrounding fluid.

VI. SUMMARY

In this paper we have examined the dynamics of flat, viscoelastic membranes either immersed in a viscous Newtonian fluid, or separating two Newtonian fluids of differing viscosities. We have paid particular attention in this analysis to dynamical issues related to microrheological measurements. Thus, we have calculated in some detail the correlated fluctuation spectrum of two rigid particles embedded in the
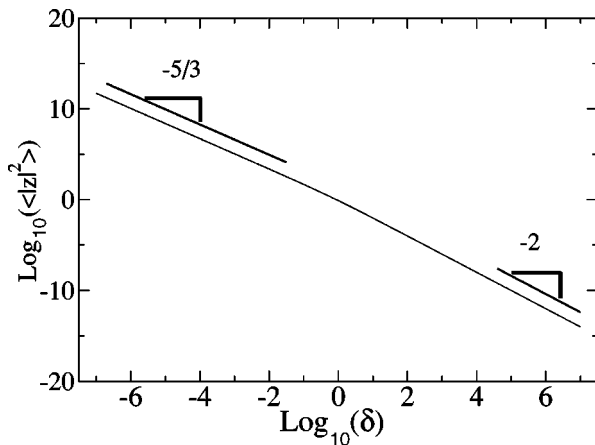
FIG. 6. The out-of-plane tracer particle fluctuation spectrum in arbitrary units plotted against a dimensionless frequency. See the definition of δ immediately following Eq. (39). At low frequencies, where the dynamics of the tracer is dominated by the membrane bending stiffness, the $-5/3$ power law is obtained. At high frequencies where the fluid viscosity dominates the dynamical response of the particle, this power law crosses over to the -2 exponent, which is expected for the Brownian motion of a free particle.

membrane. In addition, we have computed the response function of a single particle in such a membrane. Both of these calculations can be directly applied to the analysis of experimental data, whether it be from an actual linear response measurement of the force-position response of a tracer particle (e.g., with magnetic particles, or laser tweezers) or from the measurement of the autocorrelations or interparticle correlations of tracer particles undergoing thermal, Brownian motion on the membrane. In addition, the general response functions can be used to calculate the full flow and displacement fields in the membrane and fluid for a variety of extended objects embedded in viscoelastic films.

The range of applications is quite large. At the moment we restrict the equilibrium shape of the viscoelastic membrane to be flat, although we expect the results in this paper to be applicable to curved systems as long as the particle motion and interparticle separation in the case of the two-particle measurements remain small compared to the radius of curvature. The above work can be applied to lamellar phases in aqueous surfactant systems, lipid bilayers, emulsion droplets, ''polymersomes'' (as long as they are large enough—see the above comments regarding curvature), Langmuir monolayers, and cell membranes. In some of these

cases, and especially the latter, surface tension will play a significant role. This effect can be incorporated by including a term of the form γq^2, in addition to κq^4 in, for example, Eq. (38), where γ is the surface tension.

A number of extensions of this work are both possible and interesting to pursue. The first is to study the role of equilibrium (background) membrane curvature on the dynamics. Since it is already known that there is a purely geometric coupling between in-plane strains and out-of-plane bending modes, one should find a rich structure in the cross correlations of in-plane and out-of-plane motion resulting from the interplay of the geometric and hydrodynamic couplings of these modes. In addition, such an analysis is necessary to extend the methods of microrheology to highly curved surfaces. Other important extensions of the present theory include the analysis of the coupling of a viscoelastic membrane to a viscoelastic bulk material. The cell membrane coupled to the viscoelastic cytoplasm is an important realization of such a system.

Along the lines of applying these results to cellular microrheology, it must be noted that we have studied a one-component continuum model of the membrane, whereas the physical cell membrane is a highly heterogeneous material on the submicron length scale. It is therefore important to examine a more complex, multicomponent model for the membrane. Such more detailed dynamical models have been previously studied in the context of three-dimensional microrheology. These studies, in accord with very general arguments, have shown that there are necessarily extra dynamical modes in the heterogeneous models. However, based on the three-dimensional work, we expect that the principal effect of these extra modes will be to change the correlation spectra only at the lowest measurable frequencies.

[1] F. Brochard and J.F. Lennon, J. Phys. (Paris) **36**, 1035 (1975).

[2] E.H. Lucassen-Reynders and J. Lucassen, Adv. Colloid Interface Sci. **2**, 347 (1969).

[3] L. Kramer, J. Chem. Phys. **55**, 2097 (1971).

[4] J.L. Harden and H. Pleiner, Phys. Rev. E **49**, 1411 (1994).

[5] T. Chou, S.K. Lucas, and H.A. Stone, Phys. Fluids **7**, 1872 (1995).

[6] E. Helfer, S. Harlepp, L. Bourdieu, J. Robert, F.C. MacKintosh, and D. Chatenay, Phys. Rev. Lett. **85**, 457 (2000).

[7] E. Helfer, S. Harlepp, L. Bourdieu, J. Robert, F.C. MacKintosh, and D. Chatenay, Phys. Rev. E **63**, 021904 (2001).

[8] E. Helfer, S. Harlepp, L. Bourdieu, J. Robert, F.C. MacKintosh, and D. Chatenay, Phys. Rev. Lett. **87**, 088103 (2001).

[9] K.S. Zaner and P.A. Valberg, J. Cell Biol. **109**, 2233 (1989); F. Ziemann, J. Radler, and E. Sackmann, Biophys. J. **66**, 2210 (1994); F.G. Schmidt, F. Ziemann, and E. Sackmann, Eur.

Biophys. J. **24**, 348 (1996); F. Amblard, A.C. Maggs, B. Yurke, A.N. Pargellis, and S. Leibler, Phys. Rev. Lett. **77**, 4470 (1996).

[10] T.G. Mason and D.A. Weitz, Phys. Rev. Lett. **74**, 1250 (1995).

[11] T.G. Mason, K. Ganesan, J.H. van Zanten, D. Wirtz, and S.C. Kuo, Phys. Rev. Lett. **79**, 3282 (1997).

[12] F. Gittes, B. Schnurr, P.D. Olmsted, F.C. MacKintosh, and C.F. Schmidt, Phys. Rev. Lett. **79**, 3286 (1997).

[13] B. Schnurr, F. Gittes, F.C. MacKintosh, and C.F. Schmidt, Macromolecules **30**, 7781 (1997).

[14] F.C. MacKintosh and C.F. Schmidt, Curr. Opin. Colloid Interface Sci. **4**, 300 (1999).

[15] J.C. Crocker, M.T. Valentine, E.R. Weeks, T. Gisler, P.D. Kaplan, A.G. Yodh, and D.A. Weitz, Phys. Rev. Lett. **85**, 888 (2000).

[16] S. Yamada, D. Wirtz, and S.C. Kuo, Biophys. J. **78**, 1736 (2000).

[17] M. Valentine (private communication); C.F. Schmidt (private communication).

[18] D. Wirtz (private communication).

[19] Alex J. Levine and T.C. Lubensky, Phys. Rev. Lett. **85**, 1774 (2000).

[20] Alex J. Levine and T.C. Lubensky, Phys. Rev. E **63**, 016118 (2001).

[21] See, for example, P. M. Chaikin and T. C. Lubensky, *Principles of Condensed Matter Physics* (Cambridge University Press, New York, 1995).

[22] D.K. Lubensky and R.E. Goldstein, Phys. Fluids **8**, 843 (1996). Here an alternative approach to obtain these response functions is outlined.

[23] H.A. Stone and A. Ajdari, J. Fluid Mech. **369**, 151 (1998).

[24] H. Yoon and J.M. Deutsch, Phys. Rev. E **56**, 3412 (1997).

[25] E. Weeks and A. Yodh (private communication).

[26] Alex J. Levine and T.C. Lubensky, Phys. Rev. E **65**, 011501 (2002).

[27] B.D. Hughes, B.A. Pailthorpe, and L.R. White, J. Fluid Mech. **110**, 349 (1981).

[28] A.G. Zilman and R. Granek, Phys. Rev. Lett. **77**, 4788 (1996); R. Granek, J. Phys. II **7**, 1761 (1997).